

Measurements of Temperature and Water Vapour Concentration in a Scramjet Combustor

A. D. Griffiths¹ and A. F. P. Houwing¹

¹Department of Physics, The Faculties
The Australian National University, ACT, 0200 AUSTRALIA

Abstract

Two-line, time-multiplexed diode laser absorption spectroscopy is applied to a scramjet combustor to measure water vapour concentration and temperature at sampling rates of up to 20 kHz. The measurement is made in the supersonic, expanding exhaust region of the combustor and is shown to be repeatable and able to resolve differences between different operating conditions.

Introduction

For many years, hypersonic airbreathing propulsion has been promoted as an economical alternative to rocket propulsion for payload deployment into low earth orbit [3]. This has motivated many fundamental studies of scramjet flows (e.g. [6]), a significant number of which were undertaken in a free-piston shock tunnel [10]. Some of this earlier work used schlieren, luminosity or fluorescence imaging or floor or sidewall pressure measurements. The aim of the current work is to use a diode laser absorption technique (tunable diode laser absorption spectroscopy, or TDLAS) to measure temperature and water vapour density within a hydrogen-fueled scramjet. In so doing, we intend to make a unique contribution to fundamental scramjet research, demonstrating for the first time the viability of a diode laser absorption system for supersonic combustion measurements in a pulsed facility. In addition, we expect to provide data suitable for comparison with theoretical results produced by computational fluid dynamical (CFD) simulation of the flow within the scramjet.

Theoretical background

The application of absorption spectroscopy, using diode lasers, for thermometry and species measurement has been well established previously for environmental measurements, combustion studies and gasdynamic measurements [1]. The theory that underpins the technique is also well established (e.g. [1]) so only a brief outline of the theory is presented here.

As a monochromatic beam from a diode laser passes through an absorbing medium, the transmitted intensity of the beam, I , is related to the initial intensity, I_0 , by the Beer–Lambert relation

$$I = I_0 \exp(-k_\nu l) \quad (1)$$

where k_ν is the frequency-dependant absorption coefficient and l is the path length travelled by the beam. The product $k_\nu l = \log(I_0/I)$ is termed the spectral absorbance.

If an absorption line, of species i in some gas mixture, is sufficiently isolated from other spectral features then k_ν is a function of the strength, $S(T)$, and shape, $g(\nu)$ where $\int g(\nu) d\nu = 1$, of the absorption line and the number density, N_i , of the molecular species. This relation is given by

$$k_\nu = S(T) g(\nu) N_i \quad (2)$$

so that k_ν , as well as depending on frequency, depends on the temperature, T . For the case of multiple overlapping spectral lines, k_ν is treated as a sum over the individual spectral lines.

If $S(T)$ is known, then equation (2) can be used to find N_i by integrating absorbance over frequency. This requires knowledge of the temperature, which can be found by probing a second absorption line.

Thermometry relies on the dependence of line strength on temperature [8],

$$S(T) = S(T_0) \frac{Q(T_0) \exp(-c_2 E''/T)}{Q(T) \exp(-c_2 E''/T_0)} \times \frac{[1 - \exp(-c_2 \nu_0/T)]}{[1 - \exp(-c_2 \nu_0/T_0)]} \quad (3)$$

where the line strength measured at a reference temperature, $S(T_0)$ is scaled to an arbitrary temperature T . This scaling function depends on the lower-state energy of the transition, E'' , the frequency of the transition, ν_0 , and the total internal partition sum of the molecule, Q , which can be computed using the method of Fischer *et al.* [2]. Also appearing in the expression is the second radiation constant, $c_2 = hc/k$ where h is Planck's constant, c is the speed of light and k is Boltzmann's constant.

From equation (3) we see that if we choose two spectral lines of different E'' and similar ν_0 then the ratio

$$R(T) = \frac{S_1(T)}{S_2(T)} = \frac{S_1(T_0)}{S_2(T_0)} \exp \left[-c_2 (E''_1 - E''_2) \left(\frac{1}{T} - \frac{1}{T_0} \right) \right] \quad (4)$$

is a function only of T . Therefore, if an experimental system is arranged in such a way so as to measure the integrated spectral absorption of two spectral lines with different lower-state energies then both temperature and species concentration can be deduced. Furthermore, the sensitivity of the thermometry can be tuned to a particular temperature range by choosing spectral lines with appropriate E'' .

Experimental Configuration

The experimental system that was built for this purpose is shown in figure 1. Two diode lasers (Laser Components SPECILAS DFB diodes operating near 1390 nm) produced the probe beam for the system. These diodes exhibit narrow line width and no mode hops were observed in the tuning range. The laser frequency was tunable across around 10 cm^{-1} by controlling the temperature and injection current of the laser. Temperature control was used to tune the lasers into the region of a target absorption line and then current modulation was used to scan the two lasers alternately across approximately 0.5 cm^{-1} . Current modulation allowed for a repetition rate of up to 20 kHz, but meant that the laser power varied by a factor of two over a scan. Modulation was applied to the external modulation input of the diode laser controllers (ILX LDC 3700B).

The first laser was tuned to a water vapour absorption line at $7181.15570 \text{ cm}^{-1}$ while the second laser was tuned to a line at $7179.7519 \text{ cm}^{-1}$. The second line is around 70 times weaker than the first at room temperature with this ratio dropping as temperature increases. The strength of the line near 7181 cm^{-1} at room temperature necessitated flushing of the exposed beam

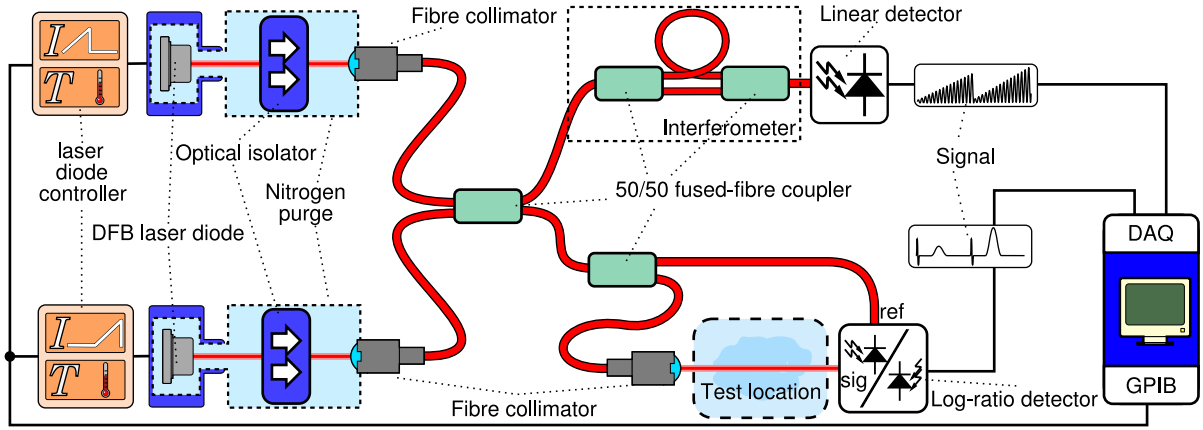


Figure 1: Experimental layout.

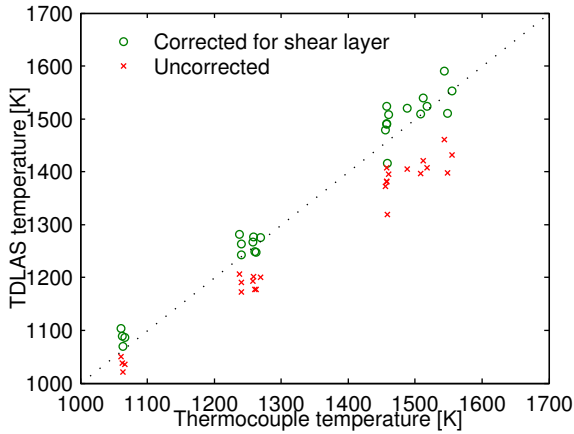


Figure 2: Temperature in a flame measured with a thermocouple compared with TDLAS. Systematic deviations are visible if a homogeneous beam path is assumed but temperature agrees well if the line-of-sight profile is specified.

path with a purge gas (nitrogen). This purge region was not very large since the beam was coupled into fibre-optics after leaving the laser housing and passing through an optical isolator.

The fibre-optic network then delivered the beam to the measurement location—the scramjet combustor or, during calibration, a flat flame burner—and to a fibre-optic interferometer which measured the relative frequency of the laser as it was scanned across the absorption line.

The remaining component of the laser light was split again with half going to the reference channel of a log-ratio detector and half passing through the test area to the signal channel of the detector. This detector [4] has been used previously for diode laser absorption spectroscopy [1] because of its ability to suppress the modulation of laser power due to injection current modulation, among other useful features. It produces a voltage

$$V = -G \log(I_{\text{ref}}/I_{\text{sig}} - 1), \quad (5)$$

where G is the gain of the detector and I_{ref} and I_{sig} are the reference and signal photocurrents respectively, which is readily converted to absorbance. The detector exhibits the best bandwidth and noise characteristics when the output voltage is adjusted to be around 0V, which is achieved when $I_{\text{ref}} \approx 2I_{\text{sig}}$.

After losses through the fibre optic network, $I_{\text{sig}} \approx 100 \mu\text{W}$ near the centre of a scan.

The output of the balanced detector and the interferometer were digitised with a PC based data acquisition board (National Instruments PCI-6110E) at 5MS/s then processed to obtain the spectral absorbance, $k_{\nu}l$, as a function of frequency. Spectral lines were then fit to this data, using the Voigt line shape for $g(\nu)$ in equation (2), thereby obtaining R .

This process was complicated by the appearance of an additional spectral line at high temperature. This line was not predicted by the HITRAN database and overlapped the line near 7181 cm^{-1} . To compensate for this, a two-line fit was used for the 7181 cm^{-1} region with the value of S_{7181} taken from the strength fitted to the original, target line.

Before deployment to the tunnel, the system was tested in a premixed burner [7] and where temperature was measured with an S-type thermocouple. The thermocouple temperature was corrected for radiation losses, a correction of up to 30K. Best results were obtained by using reference strengths, $S(T_0)$, measured by Toth [11] and then using parameters in the 2000 edition of the HITRAN database [9] to scale the strengths with temperature. The TDLAS temperature also required a correction since the beam passed through the cooler shear layer of the flame. This was applied by measuring the flame temperature profile with a thermocouple traverse, assuming that the shape of this distribution was constant and modelling the water vapour concentration based on the temperature distribution.

When this correction was applied, the comparison between thermocouple and TDLAS temperature was good, as shown in figure 2. While the assumption of homogeneous properties along the beam path results in a systematic offset that increases with temperature, the systematic error is below 1% when the above-mentioned correction was applied.

Following determination of the temperature, equation (3) can be used to find the strength of either of the two absorption lines and equation (1) applied to find the water vapour concentration. If temperature is determined in this way, either of the two absorption lines can be used to produce the same numerical result.

Scramjet measurements

Flow facility and scramjet model

Measurements using diode laser absorption spectroscopy were carried out in a model scramjet in the T3 shock tunnel at the

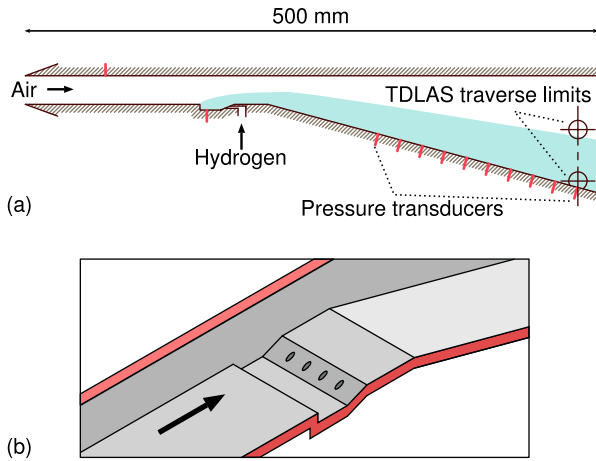


Figure 3: The scramjet model used in these experiments. Part (a) shows the duct cross section, including a sketch of water vapour distribution. The cavity geometry, with injector ports, is shown in (b).

Australian National University. This facility [5, 10] can produce flow conditions to simulate hypersonic flight, but the test duration, at around 3 ms, is short. Apart from modifications to the downstream geometry—a diverging duct instead of a straight duct—and addition of TDLAS equipment, this work used the same scramjet model and flow conditions as Neely *et al.* [5]. This model was developed for combustor studies and, therefore, does not include an intake. As a result, the tunnel was configured to produce the conditions, shown in table 1, that would be present after the intake of a hypersonic vehicle in flight.

Temperature	1160 ± 50 K
Pressure	80 ± 6 kPa
Velocity	2790 ± 30 ms ⁻¹
Density	0.23 ± 0.01 kgm ⁻³
Mach number	4.16 ± 0.09

Table 1: Conditions at the combustor intake at 1.5 ms. These are nominally the same as ref [5] and representative of a vehicle flying at around Mach 10.

After leaving the contoured nozzle of T3, the main flow entered the scramjet combustor, shown in figure 3. It first traveled down a rectangular duct of height 25 mm and width 52 mm until reaching a cavity in the floor of the duct. The cavity was designed to produce a recirculation zone for flame-holding, and hydrogen was injected into the cavity from four injector ports in the sloping rear face. Temperatures in this part of the duct were high enough for self-ignition of the fuel–air mixture, initiating water vapour production. The rate of hydrogen injection was set by the desired fuel–oxygen equivalence ratio [5]. For this work two fuel-lean equivalence ratios were used, ‘high’ with $\phi = 0.47 \pm 0.01$ at 1.5 ms and ‘low’ with $\phi = 0.153 \pm 0.005$ at 1.5 ms where uncertainties represent the standard deviation of the shot-to-shot scatter.

Aft of the cavity, the flow was expanded by a 15° ramp in the floor of the duct. This reduced the temperature of the flow to within the range where the lines chosen for this work are effective for thermometry and reduced the pressure, increasing the peak absorption.

The laser beam for TDLAS was aligned horizontally across the scramjet duct perpendicular to the flow in this region of lower temperature. The beam could be traversed vertically across the duct covering the region where cross-flow variation in water vapour was expected—from 5.6 mm above the duct floor to 50.6 mm above the duct floor, thus accessing half of the duct’s vertical extent. The beam centre was 482 mm downstream of the scramjet inlet.

The duct was instrumented with piezoelectric PCB pressure transducers along its centreline. Pressure readings showed evidence of the presence of supersonic combustion for both equivalence ratios.

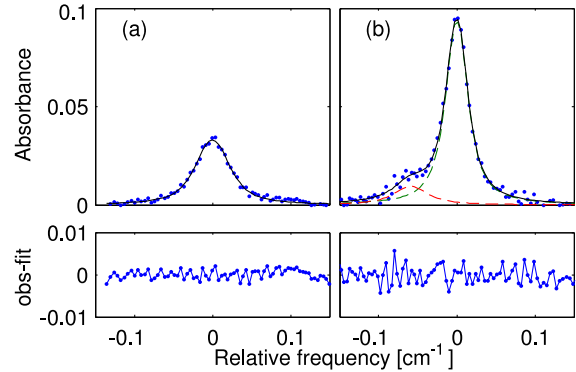


Figure 4: Single-sweep absorption data, and fits, from a high ϕ run showing (a) the line near 7179.7 cm⁻¹ and (b) the two lines near 7181 cm⁻¹ with the components shown as dashed lines.

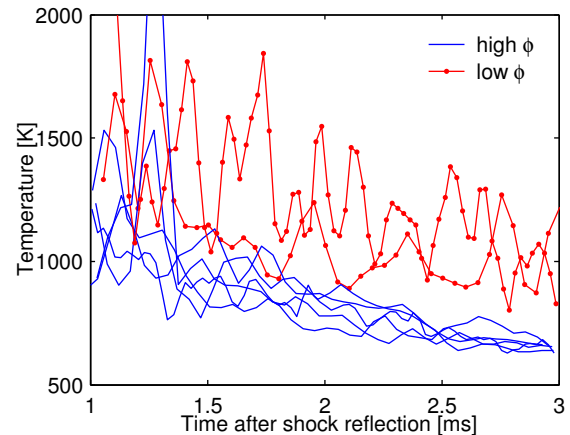


Figure 5: Temperature measured at 10.6 mm from duct floor for two different equivalence ratios.

TDLAS results

In order to test the viability of TDLAS as a diagnostic in the combustor, repeated measurements were carried out at 10.6 mm from the bottom of the duct and 482 mm from the inlet. This location was chosen after a preliminary survey of the traverse showed the presence of water vapour at a suitable temperature for thermometry.

The absorption signal measured at this location showed adequate signal-to-noise ratio and Voigt profiles showed good fits to the data. A single Voigt profile was used for the line near 7179.8 cm⁻¹, shown in figure 4 (a), while two Voigt profiles

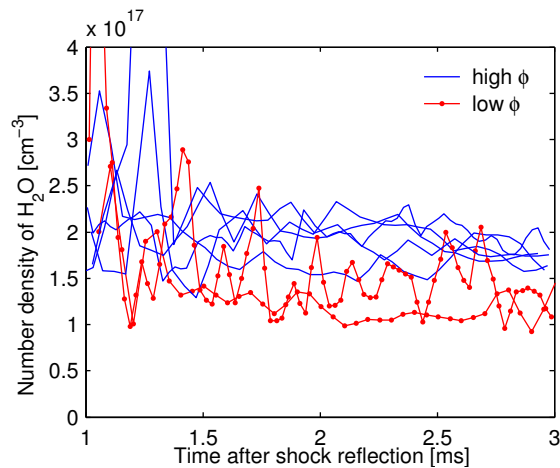


Figure 6: Water vapour number density derived from the same data set as figure 5.

were used in order to distinguish the two lines near 7181 cm^{-1} , as shown in figure 4 (b), with the stronger of these two lines being the targeted transition. The absorption lines shown are for single laser scans, since the short test time of the facility precludes averaging multiple scans, taken during a high equivalence ratio run. Similar quality of fit can be seen in runs where the equivalence ratio was low.

Processing absorption signals from multiple runs of the tunnel results in the temperature and water vapour number density as shown in figures 5 and 6 respectively. Temperature and number density histories from seven tunnel runs are plotted together with five examples of the low equivalence ratio case and two of the larger one. Most of these were acquired at 10kHz, however two were acquired at 20kHz and show equally successful operation at the higher sampling rate.

Considering the results at 2ms after shock reflection, we observe a greater concentration of water vapour when equivalence ratio is higher, as expected. The temperature variation with equivalence ratio, however, runs contrary to expectation. Furthermore, the temperature result is highly repeatable with a clear distinction between the two cases.

Within each tunnel run there is also a clear trend. The time from 1 – 3ms is within the nominal test time for these tunnel operating conditions, however no steady state is apparent in the temperature results. On the contrary, a downwards trend is apparent for both equivalence ratio cases, although a plateau may be hidden by the large variability in the measurements.

Discussion

The result here that is the most difficult to explain is the increase in temperature following a decrease in equivalence ratio. Furthermore, if we temporarily accept this relationship to hold, an explanation for the decrease in temperature over the facility test time is apparent. Over this time, while the hydrogen mass flux remains approximately constant, the air mass flux steadily decreases resulting in an increase in the equivalence ratio over the test time and, in agreement with our initial observation, a decrease in temperature.

A key to understanding why this is the case may lie in the fact that TDLAS is sensitive only at a point; possibly the hot region of the flow is moved up the duct when equivalence ratio is increased. Furthermore, if there is significant non-uniformity over

the beam path, the inferred temperature is not simply an average over the beam path due to the nonlinear relationship between temperature and line strengths. Rather, it can be weighted towards cold regions of the flow where the 7181 cm^{-1} line is particularly strong. This effect was seen to be important in flame-based calibration, and may be more pronounced in the combustor.

More work is needed in order to understand this, and CFD work is planned in the near future. Direct comparison of these results with those obtained with CFD is also expected to be instructive.

Conclusions

While interpretation remains difficult, the feasibility of using diode laser absorption spectroscopy for scramjet measurements in a pulsed facility has been established. The sampling rate achieved was high enough to indicate trends over the test time of the facility and the results were clearly different when the fuel–air equivalence ratio was varied. Planned CFD calculations should provide a better understanding of the physical processes occurring in the scramjet combustor.

References

- [1] Allen, M. G., Diode laser absorption sensors for gas dynamic and combustion flows, *Meas. Sci. Technol.*, **9**, 1998, 545–562.
- [2] Fischer, J. et al., Total internal partition sums for molecular species in the 2000 edition of the HITRAN database, *J. Quant. Spectrosc. Ra.*, **82**, 2003, 401–412.
- [3] Heiser, W. H. and Pratt, D. T., *Hypersonic Airbreathing Propulsion*, AIAA, 1994.
- [4] Hobbs, P. C. D., Ultrasensitive laser measurements without tears, *Appl. Optics*, **38**, 1997, 903–920.
- [5] Neely, A. et al., Hydrocarbon and hydrogen-fuelled scramjet cavity flameholder performance at high flight Mach numbers, in *12th AIAA International Space Planes and Hypersonic Systems and Technologies Conference*, 2003, AIAA 2003-6989.
- [6] O’Byrne, S., Doolan, M. and Houwing, A. F. P., Analysis of thermal choking processes in a model scramjet engine, *J. Propul. Power*, **16**, 2000, 808–814.
- [7] Prucker, S., Meier, W. and Stricker, W., A flat flame burner as calibration source for combustion research: Temperatures and species concentrations of premixed H_2/air flames, *Rev. Sci. Instrum.*, **65**, 1994, 2908–2911.
- [8] Rothman, L. S. et al., The Hitran molecular spectroscopic database and Hawks (Hitran Atmospheric Workstation) 1996 edition, *J. Quant. Spectrosc. Ra.*, **60**, 1998, 665–710.
- [9] Rothman, L. S. et al., The HITRAN molecular spectroscopic database: edition of 2000 including updates through 2001, *J. Quant. Spectrosc. Ra.*, **82**, 2003, 5–44.
- [10] Stalker, R. J., Development of a hypervelocity wind tunnel, *Aeronaut. J.*, **76**, 1972, 374–384.
- [11] Toth, R. A., Extensive measurements of H_2^{16}O line frequencies and strengths: 5750 to 7965 cm^{-1} , *Appl. Optics*, **33**, 1994, 4851–4863.